



RESEARCH ARTICLE

Relative entropy is an easy-to-use invasive electroencephalographic biomarker of the epileptogenic zone

Vojtech Travnicek^{1,2}  | Petr Klimes^{1,2}  | Jan Cimbalnik² | Josef Halamek^{1,2} | Pavel Jurak^{1,2} | Benjamin Brinkmann³  | Irena Balzekas³ | Chifaou Abdallah⁴ | François Dubeau⁵ | Birgit Frauscher⁴  | Greg Worrell³ | Milan Brazdil^{6,7} 

¹Institute of Scientific Instruments, Czech Academy of Sciences, Brno, Czech Republic

²International Clinical Research Center, St. Anne's University Hospital, Brno, Czech Republic

³Bioelectronics, Neurophysiology, and Engineering Laboratory, Departments of Neurology and Physiology & Biomedical Engineering, Mayo Clinic, Rochester, Minnesota, USA

⁴Analytical Neurophysiology Lab, Montreal Neurological Institute and Hospital, McGill University, Montreal, Quebec, Canada

⁵Montreal Neurological Institute and Hospital, McGill University, Montreal, Quebec, Canada

⁶Department of Neurology, Brno Epilepsy Center, St. Anne's University Hospital and Medical Faculty of Masaryk University, Brno, Czech Republic

⁷Central European Institute of Technology, Masaryk University, Brno, Czech Republic

Correspondence

Jan Cimbalnik, International Clinical Research Center, St. Anne's University Hospital, Brno, Czech Republic.
Email: jan.cimbalnik@fnusa.cz

Abstract

Objective: High-frequency oscillations are considered among the most promising interictal biomarkers of the epileptogenic zone in patients suffering from pharmacoresistant focal epilepsy. However, there is no clear definition of pathological high-frequency oscillations, and the existing detectors vary in methodology, performance, and computational costs. This study proposes relative entropy as an easy-to-use novel interictal biomarker of the epileptic tissue.

Methods: We evaluated relative entropy and high-frequency oscillation biomarkers on intracranial electroencephalographic data from 39 patients with seizure-free postoperative outcome (Engel Ia) from three institutions. We tested their capability to localize the epileptogenic zone, defined as resected contacts located in the seizure onset zone. The performance was compared using areas under the receiver operating curves (AUROCs) and precision-recall curves. Then we tested whether a universal threshold can be used to delineate the epileptogenic zone across patients from different institutions.

Results: Relative entropy in the ripple band (80–250 Hz) achieved an average AUROC of .85. The normalized high-frequency oscillation rate in the ripple band showed an identical AUROC of .85. In contrast to high-frequency oscillations, relative entropy did not require any patient-level normalization and was easy and fast to calculate due to its clear and straightforward definition. One threshold could be set across different patients and institutions, because relative entropy is independent of signal amplitude and sampling frequency.

Significance: Although both relative entropy and high-frequency oscillations have a similar performance, relative entropy has significant advantages such as straightforward definition, computational speed, and universal interpatient threshold, making it an easy-to-use promising biomarker of the epileptogenic zone.

KEYWORDS

drug-resistant epilepsy, iEEG, SOZ localization

This is an open access article under the terms of the [Creative Commons Attribution-NonCommercial](https://creativecommons.org/licenses/by-nc/4.0/) License, which permits use, distribution and reproduction in any medium, provided the original work is properly cited and is not used for commercial purposes.

© 2023 The Authors. *Epilepsia* published by Wiley Periodicals LLC on behalf of International League Against Epilepsy.

1 | INTRODUCTION

Epilepsy is one of the most prevalent diseases in the population.¹ Whereas approximately two thirds of patients respond well to antiseizure medication, the remaining one third should be considered for surgical management.² Operative removal of epileptogenic tissue provides the best chance for patients with pharmacologically intractable focal epilepsy to become seizure-free.³ To accurately determine the epileptogenic zone (EZ), many patients have to undergo implantation of intracranial electrodes. However, long-term seizure freedom is achieved in only one third of these patients.³

The current clinical gold standard for determination of the EZ uses ictal data, which are inspected visually by epileptologists.⁴ The need to record habitual seizures prolongs patients' stays in specialized video-electroencephalographic (EEG) monitoring units, increases risks for patients, and increases the workload of medical staff. To improve the outcomes of the treatment and shorten the hospitalization time, identification of reliable interictal biomarkers of the pathological area is crucial.

Among of the recognized interictal biomarkers are interictal epileptiform discharges (IEDs). Although they are known to spatially correlate with the EZ, their specificity is low.⁵ In the past 2 decades, high-frequency oscillations (HFOs) have been studied. Their higher specificity with the EZ compared to IEDs makes them a more promising interictal biomarker.⁶ Numerous studies have confirmed their association with epileptic foci,⁷ and one study reports a 100% success rate.⁸ However, the studies used grouped statistics across patient cohorts, the localization of seizure-generating tissue using HFOs in individual patients is successful in roughly two thirds of cases,^{9,10} and a recent randomized control trial claims that HFOs are not ready for clinical interpretation.¹¹ The discrepancies between studies could be ascribed to the lack of a clear definition of HFOs. This leads to high interrater variability¹² and development of a vast array of automated HFO detectors.¹³ Another limiting factor for using HFOs is that physiological HFOs occur as a result of normal cognitive processing,^{14–17} which might mask pathological HFOs and result in variations of HFO counts in individual patients.

More recently, multiple studies reported altered connectivity patterns inside the EZ compared to the non-EZ, suggesting functional connectivity as a promising new interictal biomarker.^{18,19} To date, none of the proposed connectivity measures reached the sensitivity and specificity of HFOs on a systematic and representative data sample.^{20,21}

Another approach is to quantify the level of complexity of physiological signals, because disease degrades the physiological function and therefore decreases signal complexity.²² Costa et al.²³ suggest a multiscale entropy measure, which was successfully used to localize the

Key Points

- Relative entropy localizes the epileptogenic zone with the same performance as high-frequency oscillations
- Relative entropy is computationally more efficient than high-frequency oscillations
- When delineating the epileptogenic zone, relative entropy can use one threshold for all patients and keep the performance of individual thresholding

seizure onset zone (SOZ) in the dataset of 13 pediatric patients with focal cortical dysplasia.²⁴ In general, different entropy measures for localization of the EZ are used in Dauwels et al.,¹⁹ Ben-Jacob et al.,²⁵ Gazit et al.,²⁶ and Mooij et al.²⁷ These articles use various entropy measures as part of complex algorithms mostly based on time-frequency analysis and either have few patients to compare its performance to HFO or do not have comparable results.

In this study, we propose relative entropy (REN) as a novel interictal biomarker of the EZ. Our previous work showed increased linear correlation within the EZ and reduced functional connections on its edges, using “bridging contacts”—two adjacent contacts on a depth electrode.^{28,29} We hypothesize that REN calculated as a bivariate measure on adjacent contacts has the potential to reflect this phenomenon in a broader context of spectral complexity, which can provide additional information for the delineation of EZ. Our hypothesis is that REN is higher inside the EZ than in the remaining area, as a larger difference between signals is typical for more excitable pathological tissue as present in the EZ. In contrast, REN is lower in the case of more similar signals between two brain regions. Furthermore, we hypothesize that REN does not require any patient-level normalization and thus is able to provide more stable and reproducible results than HFOs.

2 | MATERIALS AND METHODS

2.1 | Patients

Three centers participated in this study: (1) Brno Epilepsy Center, St. Anne's University Hospital; (2) Mayo Systems Electrophysiology Laboratory, Mayo Clinic, Rochester; and (3) ANPHY Lab, Montreal Neurological Institute and Hospital (MNI).

The patient selection criteria for all institutions were: (1) invasive phase 2 presurgical workup with stereo-EEG (SEEG); (2) subsequent curative surgery or radiofrequency

thermocoagulation; (3) excellent outcome defined as Engel 1A or International League Against Epilepsy 1 at least 1 year after resective surgery; (4) availability of pre-surgical and postsurgical brain imaging for localization of electrode contacts and resection cavity; (5) at least one contact that was resected in the clinically marked SOZ; and (6) minimum sampling frequency of 2000 Hz.

Artifacts were annotated with Signalplant³⁰ software in Brno, custom-made software based on MATLAB was used for artifact annotation in Rochester, and Stellate Harmony software was used in Montreal.

2.2 | Recordings

Data from Brno were recorded with standard intracranial depth electrodes (five, 10, and 15) contact semiflexible multicontact platinum electrodes (DIXI Medical or Alcis; contact surface area = 5.02 mm² and intercontact distance = 1.5 mm). The average signal from all SEEG contacts was used as a reference. Data were initially sampled at 25 kHz and downsampled to 5 kHz. Patients from Rochester were recorded with intracranial depth electrodes (AD-Tech Medical, four and eight contact clinical depth electrodes with platinum/iridium clinical macroelectrode contacts, contact surface area = 9.4 mm² and intercontact distance = 10 mm) and subdural grids and strips (4.0-mm-diameter platinum/iridium discs [2.3 mm diameter exposed] with 10-mm intercontact distance). The original sampling frequency of 32 kHz was downsampled to 5 kHz with a 1-kHz Bartlett–Hanning window low-pass filter. An electrode mounted on the earlobe served as a reference electrode; however, all contacts were subsequently averaged to create a new common reference. Standard or homemade intracranial depth electrodes were used for invasive EEG (iEEG) at the MNI (DIXI or MNI electrodes). Recordings were sampled at 2 Hz with an epidural electrode fixed in the bone far from the suspected epileptic focus as a reference. A new reference signal was created by averaging all SEEG contacts.

Positions of electrodes were determined by coregistration of preimplant magnetic resonance imaging (MRI) with postimplant computed tomography or MRI scans with electrodes. All recordings were manually reviewed for data quality, and noisy channels were omitted from the study.

2.3 | Identification of the SOZ, resected contacts, and sleep scoring

The recordings were inspected by neurologists at the given center, and the SOZ was visually identified from all clinical seizures based on the earliest changes at seizure onset in the iEEG.³¹ Postresection imaging served for

determination of the contacts placed in the resection area. In the Brno and MNI patients, sleep was scored visually in the scalp EEG combined with electrooculography and chin electromyography in 30-s epochs by a board-certified neurophysiologist following the current guidelines of the American Academy of Sleep Medicine.

2.4 | Calculation of REN

Kullback–Leibler divergence, called REN,³² has its basis in information theory, where it is used to compare two probability distributions p_X and p_Y and is calculated as $REN = \sum p_X * \log\left(\frac{p_X}{p_Y}\right)$ (Figure 1).

REN was evaluated in 1-s nonoverlapping rolling windows across two signals, where a 10-bin signal histogram was used as a probability distribution of each signal. Testing different parameters of REN computation was done before we started the analysis. We chose a 10-bin histogram as a minimal number that will capture the amplitude variability and achieve good localization results. The window size of 1 s was chosen because of our internal pipeline, where we compute more features in this sliding window. However, we tested window sizes of .5, 1, and 10 s on the 19 patients from Brno (see Table S3), and the results showed no significant change in localization performance (all $p > .25$, Wilcoxon sign-rank test on individual area under the receiver operating curve [AUROC]). Using the equation, we computed REN between neighboring contacts on every electrode. Because REN is direction-dependent (if p_Y and p_X are swapped, REN will have a different value), we evaluated REN in both directions and took the higher value. For every adjacent pair of contacts, there were n REN values, where n is the length of the signal in seconds. These values were averaged over the whole recording to have one value for every pair. To evaluate every contact separately, we obtained one value for every contact by averaging entropies of adjacent pairs. Only one value was used for the first and the last contacts on an electrode. REN was calculated in the raw signal and in six frequency bands (1–4 Hz, 4–8 Hz, 8–12 Hz, 12–20 Hz, 80–250 Hz, 250–600 Hz), calculated by third order bandpass Butterworth filter. Each frequency was evaluated separately. We skipped the gamma frequency band (30–70 Hz) because of power line noise, which varies between institutions and therefore could not be processed equally.

2.5 | Detection of HFOs

Navarrete et al.¹³ compared 19 HFO detectors. If we omit the worst and the best detector, their sensitivity varied

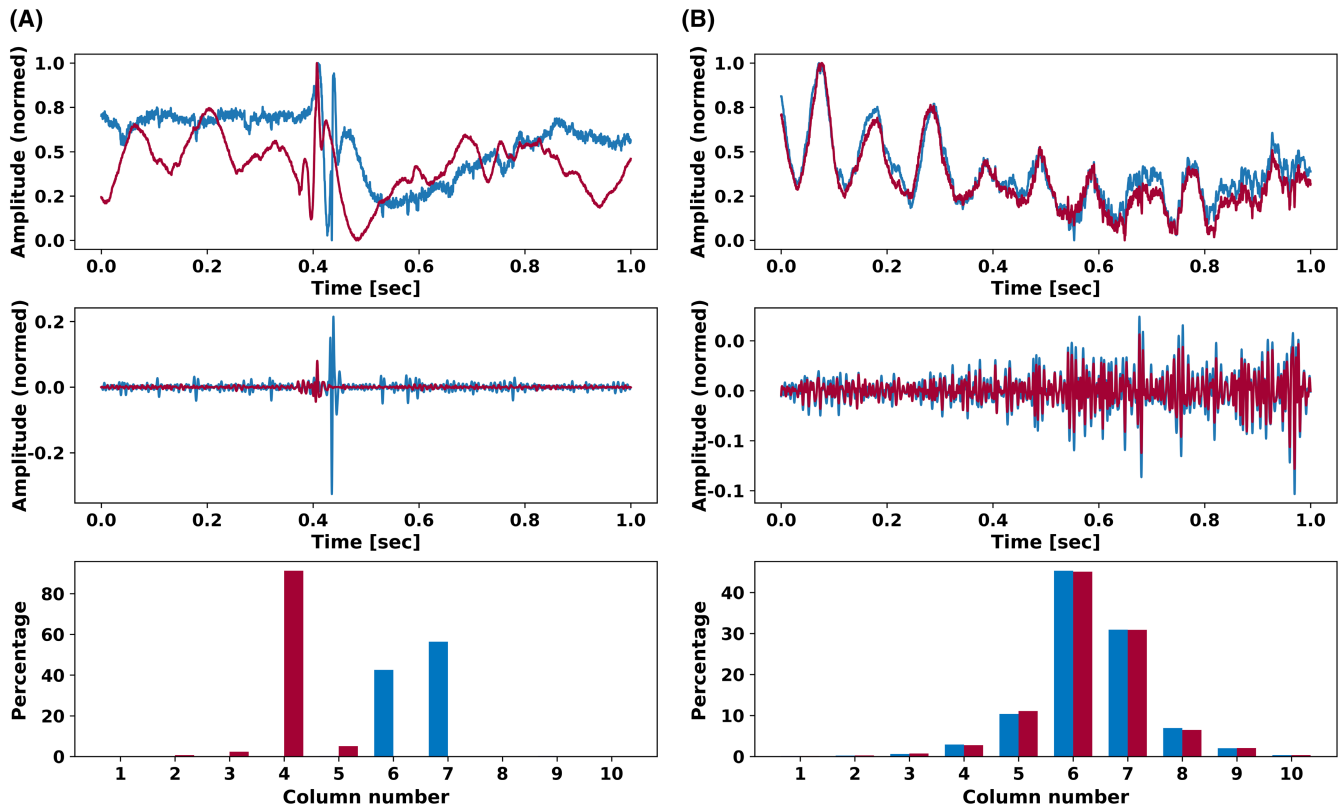


FIGURE 1 Explanation in two columns (column A, column B) of how entropy of two signals from adjacent contacts was calculated. The first row shows two signals that are being compared; in the second row, the input signals were filtered by a bandpass Butterworth filter (80–250 Hz). The third row illustrates the similarity of histograms of filtered signal amplitudes ordered from 1 to 10. These histogram values represent probability distributions that are used as inputs of the relative entropy (REN) equation. REN of Column A is 7.92, whereas REN of the signals in Column B is $<10^{-3}$.

between 74.4% and 93%. Different HFO detectors work differently at different centers. We chose the line-length (LL) detector, because we have a good experience with this algorithm at our center, it showed a sensitivity of 89.5% in the previously cited work,¹³ and it seemed a fair choice for the purpose of our comparison.

The LL detector³³ was used to detect HFOs in the ripple band (80–250 Hz) and fast ripple band (250–800 Hz). The following parameters were chosen as an input for this algorithm: statistical window of 10 s; 3 (Brno, Montreal) or 6 (Rochester) SDs as the detection threshold; and window size calculated as $(5/\text{low_fc}) * \text{fs}$ samples, where *low_fc* stands for low cutoff frequency and *fs* for sampling frequency. Window overlap was set to 25% of the sliding window length. Detection thresholds were determined individually for each institution by visually verifying the detections on three random patients. For each of these three patients, we detected HFOs with five different thresholds and manually reviewed the detections. Based on the manual review, we chose the best threshold for each site. The final HFO count for every contact was divided by the recording length in minutes to compensate for different recording lengths, so that we obtained one HFO rate for each contact.

2.6 | Statistical analysis

Epileptogenic tissue (localization target) defined as SOZ contacts overlapped with resected contacts in patients with excellent postsurgical outcomes.²⁷ Thus, elements in the confusion matrix were defined as following:

True positive: Contact that was both SOZ and resected, marked as epileptogenic.

False positive: Contact that was either only resected, only SOZ, or neither of these, marked as epileptogenic.

True negative: Contact that was either only resected, only SOZ, or neither of these, marked as healthy.

False negative: Contact that was both SOZ and resected, marked as healthy.

The algorithms were evaluated using the AUROC and the area under the precision-recall curve (AUPRC) in two ways. A combination of these two statistical measures was used to compensate for imbalanced datasets (the localization target comprises only $7.9\% \pm 5.6\%$) that can lead to overly optimistic results. First, to evaluate the capability of each feature to localize epileptogenic tissue individually

in a single patient, the curves were constructed for each patient individually resulting in one receiver operating curve (ROC) and one precision-recall curve (PRC) per patient. Final AUROC and AUPRC values for every feature were calculated by averaging patient-specific values over patients. We also used patient-specific AUROC values for every feature as the input to the Wilcoxon signed-rank test and used the results to statistically compare the performance between all features. The same values were used to compare the performance between institutions using the Mann–Whitney test.

Second, to investigate whether there is one common threshold that can distinguish between physiological and epileptogenic tissue in all patients, the ROCs and PRCs were constructed for each feature using all contacts from all patients, resulting in one PRC and one AUC per feature. From the unnormalized ROC curves, we identified the ideal threshold providing maximal values of the subtraction of the true positive rate (tpr) and false positive rate (fpr).

This approach was repeated with per patient z-score normalization and normalization with function $x/70$ th percentile. The 70th percentile was chosen to mitigate the influence of outliers. The purpose of this demonstration is to simulate the delineation of epileptogenic tissue prospectively, without any prior knowledge of SOZ or resected contacts, using a common feature threshold for all patients.

In this study, we included three different institutions, which differ in protocols, electrodes, amplifiers, and other settings. These differences can influence the biomarker performance. Using the AUROC of individual patients, we calculated the intraclass correlation to describe how much variability was caused by the affiliation with a particular institution. Venn diagrams were constructed for the best performing REN and best performing LL features. This was done to visualize how many target contacts were detected by either of the features and how many were overlapping.

The computation time of each algorithm was tested on a subset of 10 recordings from Brno Epilepsy Center sampled at 5000 Hz. LL and REN algorithms were run on a computer with a Intel Xeon Silver 4116 processor and NVIDIA GeForce GTX 1080 Ti graphic card. Every algorithm was evaluated within bands of 80–250 Hz and 250–600 Hz. We used the graphic card for bandpass filtering and the processor (always 20 processes) for the evaluation of the given algorithm. Measured time includes bandpass filtering. We processed the whole recording and divided computational time by recording length in minutes and electrode count. In this way, we calculated the average computation time per 1 min and electrode contact. Multiplying this number by 150 (representative electrode contact count for one patient), we obtained an estimation of computation time for 1 min of a representative patient recording.

3 | RESULTS

3.1 | Patients

The final cohort consisted of 39 patients from three institutions. Demographic and clinical data for all patients are provided in [Tables S1–S3](#). In Brno, patients recorded between January 2012 and January 2020 were selected for this study. The final cohort consisted of 19 patients who met the inclusion criteria with an average \pm SD age of 36.7 ± 12.3 years, 10 males and nine females. In Rochester, patients recorded between October 2006 and May 2012 were selected. The final cohort consisted of nine patients with an average age of 37.6 ± 9.9 years, four males and five females. In Montreal, patients recorded between January 2010 and January 2018 were selected. The final cohort consisted of 11 patients with an average age of 36.4 ± 11.5 years, five males and six females. Contacts in white matter were included in the analysis. Our cohort of patients had a median of 2.4% (interquartile range = 0%–18.4%) of contacts in white matter, whereas 16 patients of 39 had no contacts in white matter (patients with electrocorticography). If we exclude EZ contacts and compare white matter contacts to healthy gray matter contacts, we found no statistically significant difference in REN ($p = .065$, Mann–Whitney).

3.2 | Datasets

The first dataset consists of recordings from 39 patients with excellent outcomes, from whom 30 min of artifact-free iEEG regardless of the state of vigilance were chosen for the analysis. The average length of the recordings was 31.26 ± 2.4 min. This dataset is labeled as the "Rest dataset" for the purpose of this study.

In the second dataset, there are only patients from the Rest dataset. Random 10-min selections of both N2 and N3 sleep were chosen for the second analysis as the vigilance states that best identify the EZ.³⁴ This dataset includes 16 patients with 10 min of continuous recordings without artifacts of both N2 and N3 sleep stages. Because sleep scoring was not available for Rochester, this dataset contains only patients from Brno and Montreal. This dataset is further referenced as the "Sleep dataset." A complete list of patients and their inclusion in datasets can be found in [Tables S1–S3](#).

3.3 | Results for the Rest dataset

The best performing features in the Rest dataset were REN (80–250 Hz) and LL (80–250 Hz). [Figure 2](#) shows

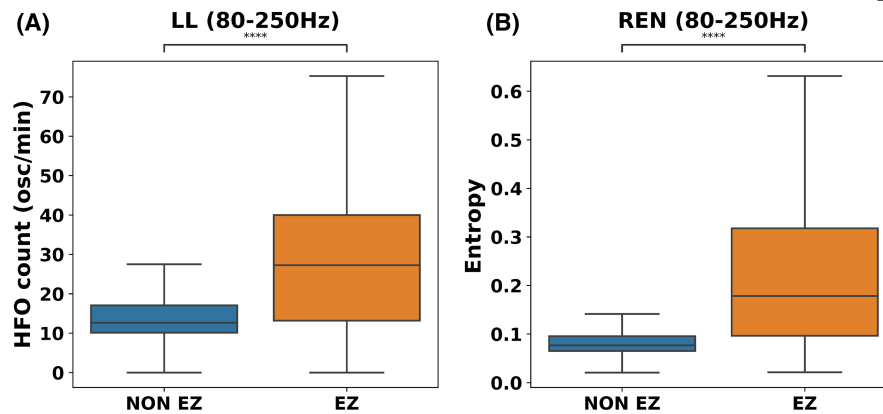


FIGURE 2 Boxplots show how the two best features differentiate between the epileptogenic zone (EZ) and non-EZ as defined in the previous section from the Rest dataset. (A) Line-length (LL; 80–250 Hz); the y-axis shows oscillation count (osc) per minute. (B) Relative entropy (REN); the y-axis has no units. The boxes show the quartiles of the dataset, and the whiskers extend to show the rest of the distribution. Outliers are not visualized. HFO, high-frequency oscillation. **** $p < .0001$.

how these features behave in the EZ versus non-EZ. Both features show low means and low variances in the non-EZ, whereas in the EZ both means and variances are increased. The significance of the distribution difference between non-EZ and EZ channels was confirmed by a Mann–Whitney test. Both LL (80–250 Hz) and REN (80–250 Hz) have $p < .001$; effect size was measured by Cliff delta and was large ($d = .64$) in the case of REN and medium ($d = .47$) in the case of LL. The percentage of target channels (as defined in the previous section) varies from 1.19% to 30.51%, with a mean value of $6.9\% \pm 5.6\%$. The intraclass correlation was 6.21% for LL (80–250 Hz) and 2.24% for REN (80–250 Hz).

REN (80–250 Hz) and LL (80–250 Hz) both have an average AUROC of .85. There was no significant difference in performance between these two features and REN (250–600 Hz, $p > .05$). LL (250–600 Hz) performed significantly worse ($p < .05$, Wilcoxon sign-rank on AUROC values). Frequency ranges 1–4 Hz, 4–8 Hz, 8–12 Hz, and 12–20 Hz were not suitable for delineating the epileptogenic tissue, because their performance was significantly worse than any of the leading features ($p < .01$). There was no significant difference in any feature performance across institutions ($p > .05$). All the feature results at all three institutions are shown in Figure 3. A statistical comparison between feature performance is provided in Figure 4.

We constructed one ROC for every feature by applying one threshold that was common for all patients. The left panel in Figure 5 shows ROCs constructed for the five best performing features. Applying one common threshold instead of the patient-specific one decreased the performance of every feature. The ideal threshold for REN (80–250 Hz) was .116, providing tpr-fpr of .54. For LL (80–250 Hz), the ideal threshold was 21.7 oscillations per minute, providing tpr-fpr of .5. The best performing

features were REN (80–250 Hz) and REN (250–600 Hz), with AUROC of .82 and .77.

Subsequently, we applied patient-specific normalization. Whereas there was no significant difference between normalized and unnormalized REN features, the LL feature performance increased significantly in both frequency bands when applying normalization ($p < .01$).

We localized target contacts using a common threshold for all patients without patient-specific normalization. Of 219 target contacts, the LL algorithm localized 157 true positives and REN localized 166 true positives. Whereas 128 target contacts were localized by both features, 38 contacts were localized only by the REN feature and 29 contacts were localized only by the LL feature. Twenty-four pathological contacts remained unlocalized.

3.4 | Results for the Sleep dataset

Results for the Sleep dataset are similar to those in the Rest dataset. The best performing features are LL (80–250 Hz) and REN (80–250 Hz). Unlike the Rest dataset, there is a significant interinstitutional difference in AUROC performance between Brno and Montreal patients ($p < .05$). AUROC and AUPRC results for all features and institutions are shown in Figure 6.

For LL (80–250 Hz), the effect of normalization decreased the AUROC from .85 to .82; however, the Wilcoxon signed-rank test did not prove significance ($p > .05$). For REN (80–250 Hz), the normalization increased AUROC from .83 to .84, but it was not significant either ($p > .05$). The ideal threshold for REN (80–250 Hz) was .102 and for LL (80–250 Hz) was 21.2 oscillations per minute.

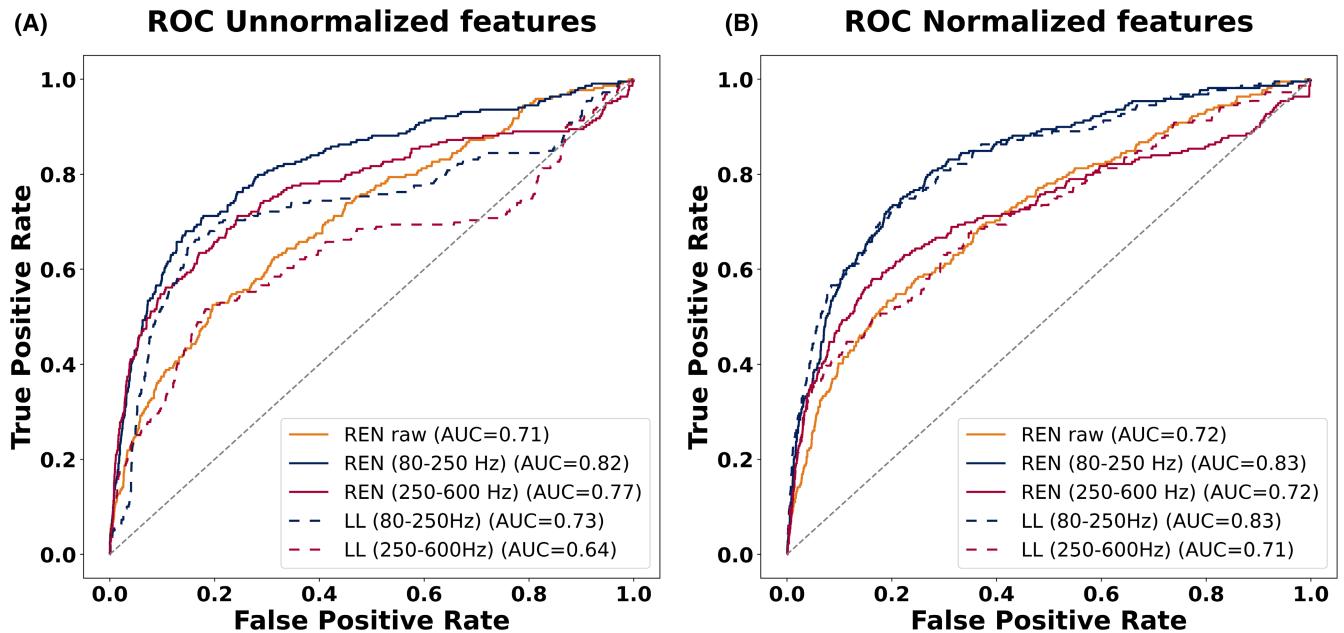


FIGURE 5 Receiver operating curves (ROCs) are constructed for all patients together. (A) ROCs constructed from unnormalized data. (B) For the construction of ROCs, z -score normalization was performed for each patient individually. Relative entropy (REN) performs well regardless of normalization, whereas the line-length (LL) algorithm was influenced by normalization, showing significantly worse performance on unnormalized data ($p < .05$). AUC, area under the curve.

	All		Brno N2		Brno N3		Montreal N2		Montreal N3	
	AUROC	AUPRC	AUROC	AUPRC	AUROC	AUPRC	AUROC	AUPRC	AUROC	AUPRC
REN raw	0.77	0.26	0.85	0.20	0.83	0.13	0.75	0.32	0.72	0.29
REN (1-4 Hz)	0.62	0.16	0.68	0.11	0.74	0.09	0.59	0.19	0.58	0.18
REN (4 - 8 Hz)	0.66	0.21	0.75	0.24	0.75	0.13	0.62	0.23	0.62	0.20
REN (8-12 Hz)	0.64	0.18	0.68	0.17	0.69	0.14	0.60	0.19	0.62	0.18
REN (12-20 Hz)	0.72	0.22	0.75	0.21	0.82	0.12	0.68	0.24	0.70	0.26
REN (80-250 Hz)	0.87	0.47	0.87	0.26	0.78	0.12	0.89	0.59	0.89	0.60
REN (250-600 Hz)	0.84	0.40	0.81	0.14	0.81	0.12	0.85	0.54	0.85	0.50
LL (80-250Hz)	0.86	0.47	0.84	0.23	0.75	0.12	0.90	0.63	0.88	0.59
LL (250-600Hz)	0.78	0.34	0.75	0.17	0.69	0.11	0.82	0.45	0.78	0.41

FIGURE 6 Averaged area under the receiver operating curve (AUROC) and area under the precision-recall curve (AUPRC) values across individual patients in the Sleep dataset. Results are visualized for institution and sleep stage separately (Brno and Montreal, N2 and N3). 'Column all averages every AUROC and AUPRC value in the row'. LL, line-length; REN, relative entropy.

different approaches in detection, often requiring raw signal normalization. We previously showed that a combination of multiple interictal features achieves superior performance to individual biomarkers.³⁶ Therefore, new interictal biomarkers carrying complementary information to those already known are needed to provide accurate information and interpatient stability for automatic algorithms providing delineation of epileptogenic tissue across institutions.

Previous studies proved functional isolation of the EZ with neighboring tissue,^{29,31} suggesting the analysis of these bridging areas to improve the localization and delineation of the EZ. Any univariate feature, including HFOs, has limited potential to capture these changes within, and around, the epileptogenic region. REN, on the other hand, is a bivariate feature, and as such it captures relationships between two areas of the brain and the corresponding neuronal assemblies. In general, REN evaluated within the EZ

is much higher than REN within healthy tissue. Entropy in general reflects the spectral complexity of the signal. A flat, white-noise-like-looking spectrum has higher entropy in contrast to a spectrum with distinct peaks. Increased REN is then observed when there are differences in spectral contents of two signals—in our case, two adjacent contacts on a depth electrode. We hypothesize that REN has the potential to reflect the bridging phenomena of the EZ in a context of spectral richness of analyzed signals, which can provide additional information for the delineation of EZ.

This study proposes REN as a novel bivariate biomarker for the localization of epileptic tissue in patients suffering from pharmacoresistant focal epilepsy. It has a clear and simple definition and, thanks to its independence on signal amplitude and sampling frequency, does not require any complex signal preprocessing or within-patient normalization. That allows for the determination of a general threshold setting across different recordings, patients, and institutions with different signal characteristics caused by different recording conditions, types of electrodes, hardware filters, A/D converter parameters, and sampling frequencies.

In practice, having a general threshold differentiating between physiological and epileptogenic tissue allows fully automatic prospective presurgical evaluation, while preserving high performance. A method that can be universally applied across institutions has the potential to contribute significantly to the creation of a general model. The generalizability of a model is still one of the major challenges in the current endeavor to automatically localize the EZ. Many proposed automatic methods for EZ localization are developed, trained, and tested on datasets from a single center³⁴ or retrained on recordings from a different center with different input parameters.³⁶ Development of a model that would not require retraining and resetting of detection thresholds is of great importance, and mandatory in order to make these algorithms ready for primetime in clinical practice.

REN fulfills these criteria. Our conclusions are derived from statistical tests on 39 patients with seizure-free postsurgical outcomes from three independent institutions. Although these institutions have different recording hardware and protocols, the intraclass correlation showed that only <10% of result variability was caused by affiliation with a particular institution. We have found that REN achieves similar results as HFOs regardless of the state of vigilance, and shows stable results across three sites while having a shorter computation time. For comparison with REN, we chose the LL HFO detector³³ for its wide use across multiple studies, straightforward methodology, and computational efficacy. Using our custom Python scripts, REN showed faster processing times than the LL algorithm and was proved to be suitable for real-time processing.³⁷ The

best performing HFO and REN features (in ripple band) showed a high overlap of true positive cases, meaning that REN computation could be used as a surrogate for HFO detection, although it inherently carries different information about the state of the brain. Nonetheless, some of the contacts were detected exclusively by only one of the two algorithms, which allows use of REN as a complementary iEEG feature to HFO detection, combining both results in machine learning models to achieve superior results.^{34,36}

Lack of comparison of REN with different HFO detectors might be considered a limitation of this study. However, to date, there is no clear definition of pathological HFOs.⁷ Many HFO detectors have been developed in the past 2 decades¹³ and typically, each center uses its own HFO detector or whichever works the best on its recordings. The overall performance of individual HFO detectors is, however, not significantly different when tuned to the optimal parameters.^{33,38,39}

EZ definition is ambiguous. For the purpose of this study, we defined the EZ as resected SOZ contacts in patients with excellent postsurgical outcomes. This approach was selected based on previous results in Cimbalnik et al.,³⁶ where the definition of the EZ as resected SOZ contacts achieved the best results in comparison with EZ defined as SOZ contacts or EZ defined as resected contacts in patients with excellent postsurgical outcome. A limitation of this approach might be in the evaluation of false positive (in the case of a non-SOZ contact that was resected, marked as pathological) and true negative (in the case of a non-SOZ contact that was resected, marked as healthy). The tissue surrounding these contacts can potentially be either healthy or pathologic. On the other hand, this limitation is the same for both methods. Therefore, HFO and REN results are influenced by the same bias.

The results in this study are derived from 30 min of relaxed recordings without the definition of the state of vigilance and 10 min of N2 and N3. Significant variability was proved in the case of HFO rates in long recordings.^{40,41} Although our results do not prove any differences in the performance between Rest and Sleep datasets, a more comprehensive analysis of continuous recordings would be needed to test for the stability of individual methods.

In conclusion, the proposed REN biomarker shows promising results for localization of epileptogenic tissue with a similar performance to the localization potential of HFO but the great advantage that it does not require any signal normalization of the patient level or threshold selection. Our results suggest that REN can be used as a surrogate for HFO or as its complement.

AUTHOR CONTRIBUTIONS

Vojtech Travnicek: Data analysis, manuscript, figures. Petr Klimes: Data acquisition in Montreal, study conception.

Jan Cimbalnik: Data acquisition in Brno, study conception. Josef Halamek: Data analysis design. Pavel Jurak: Study conception. Benjamin Brinkmann: Data acquisition in Rochester. Irena Balzekas: Gathering information on patients in Rochester. François Dubeau: Data acquisition in Montreal. Chifaou Abdallah: Gathering information on patients in Montreal. Greg Worrell, Milan Brazdil, Birgit Frauscher: Mentoring.

ACKNOWLEDGMENTS

The Czech part was supported by the Czech Health Research Council of the Ministry of Health of the Czech Republic (project AZV NU22-08-00278), the Czech Science Foundation (projects GACR 22-28784S and 21-25953S), the CAS (project RVO:68081731), the European Regional Development Fund (project ENOCH No.CZ.02.1.01/0.0/0.0/16_019/0000868), and the Ministry of Education, Youth, and Sports of the Czech Republic (MEYS; project LX22NPO5107), financed by the European Union–Next Generation EU. At the US site, the research was primarily funded by NIH R01 NS092882. In Canada, this work was primarily supported by a project grant from the Canadian Institutes of Health Research (PJT-175056). B.F. is supported by a salary award (Chercheur-boursier clinicien Senior) from the FRQS (2021–2025). We appreciate the contributions of our patients and thank the Mayo Clinic patient coordination research team (Karla Crockett, Cindy Nelson). We also wish to express our gratitude to the staff and technicians at the EEG Department of the Montreal Neurological Institute and Hospital, particularly Lorraine Allard, Nicole Drouin, and Chantal Lessard. The research was supported by the MEYS project Inter-excellence LTAUSA18.


CONFLICT OF INTEREST STATEMENT

G.W. is named inventor for intellectual property developed at Mayo Clinic and licensed to Cadence Neuroscience and NeuroOne. The authors declare no conflicts of interest. The work is consistent with the Journal's guidelines for ethical publication. All coauthors have been substantially involved in the study and/or the preparation of the manuscript. No undisclosed persons have had a primary role in the study. All coauthors saw and approved the submitted version of the paper and accept responsibility for its content.

ORCID

Vojtech Travnicek  <https://orcid.org/0000-0002-5846-6722>

Petr Klimes  <https://orcid.org/0000-0002-0232-9518>

Benjamin Brinkmann  <https://orcid.org/0000-0002-2392-8608>

Birgit Frauscher  <https://orcid.org/0000-0001-6064-1529>

Milan Brazdil  <https://orcid.org/0000-0001-7979-2343>

REFERENCES

- Leonardi M, Ustun TB. The global burden of epilepsy. *Epilepsia*. 2002;43(Suppl 6):21–5.
- Wiebe S, Blume WT, Girvin JP, Eliasziw M. A randomized, controlled trial of surgery for temporal-lobe epilepsy. *N Engl J Med*. 2001;345:311–8. <https://doi.org/10.1056/nejm200108023450501>
- Télliez-Zenteno JF, Moien-Afshari F, Hernández-Ronquillo L, Griebel R, Sadanand V. Reasons for reoperation after epilepsy surgery: a review based on a complex clinical case with three operations. *Neuropsychiatr Dis Treat*. 2010;6:409–15.
- Van Gompel JJ, Worrell GA, Bell ML, Patrick TA, Cascino GD, Raffel C, et al. Intracranial electroencephalography with subdural grid electrodes: techniques, complications, and outcomes. *Neurosurgery*. 2008;63(3):498–505. discussion 505–6.
- de Curtis M, Avanzini G. Interictal spikes in focal epileptogenesis. *Prog Neurobiol*. 2001;63(5):541–67.
- Bragin A, Engel J, Wilson CL, Fried I, Buzsáki G. High-frequency oscillations in human brain. *Hippocampus*. 1999;9:137–42. [https://doi.org/10.1002/\(sici\)1098-1063\(1999\)9:2<137::aid-hipo5>3.0.co;2-0](https://doi.org/10.1002/(sici)1098-1063(1999)9:2<137::aid-hipo5>3.0.co;2-0)
- Frauscher B, Bartolomei F, Kobayashi K, Cimbalnik J, van't Klooster MA, Rampp S, et al. High-frequency oscillations: the state of clinical research. *Epilepsia*. 2017;58(8):1316–29.
- Fedele T, Burnos S, Boran E, Krayenbühl N, Hilfiker P, Grunwald T, et al. Resection of high frequency oscillations predicts seizure outcome in the individual patient. *Sci Rep*. 2017;7(1):13836.
- Cimbalnik J, Brinkmann B, Kremen V, Jurak P, Berry B, Gompel JV, et al. Physiological and pathological high frequency oscillations in focal epilepsy. *Ann Clin Transl Neurol*. 2018;5(9):1062–76.
- Jacobs J, Wu JY, Perucca P, Zelmann R, Mader M, Dubeau F, et al. Removing high-frequency oscillations: a prospective multicenter study on seizure outcome. *Neurology*. 2018; 91(11):e1040–52.
- Zweiphenning W, Klooster MA, van Klink NE, Leijten FS, Ferrier CH, Gebbink T, et al. Intraoperative electrocorticography using high-frequency oscillations or spikes to tailor epilepsy surgery in The Netherlands (the HFO trial): a randomised, single-blind, adaptive non-inferiority trial. *Lancet Neurol*. 2022;21(11):982–93.
- Spring AM, Pittman DJ, Aghakhani Y, Jirsch J, Pillay N, Bello-Espinosa LE, et al. Interrater reliability of visually evaluated high frequency oscillations. *Clin Neurophysiol*. 2017;128(3):433–41.
- Navarrete M, Pyrzowski J, Corlier J, Valderrama M, Le Van Quyen M. Automated detection of high-frequency oscillations in electrophysiological signals: methodological advances. *J Physiol Paris*. 2016;110(4 Pt A):316–26.
- Matsumoto A, Brinkmann BH, Matthew Stead S, Matsumoto J, Kucewicz MT, Marsh WR, et al. Pathological and physiological high-frequency oscillations in focal human epilepsy. *J Neurophysiol*. 2013;110(8):1958–64.
- Kucewicz MT, Cimbalnik J, Matsumoto JY, Brinkmann BH, Bower MR, Vasoli V, et al. High frequency oscillations are associated with cognitive processing in human recognition memory. *Brain*. 2014;137(Pt 8):2231–44.
- Guragain H, Cimbalnik J, Stead M, Groppe DM, Berry BM, Kremen V, et al. Spatial variation in high-frequency

- oscillation rates and amplitudes in intracranial EEG. *Neurology*. 2018;90(8):e639–46.
17. Frauscher B, von Ellenrieder N, Zelmann R, Rogers C, Nguyen DK, Kahane P, et al. High-frequency oscillations in the Normal human brain. *Ann Neurol*. 2018;84(3):374–85.
 18. Bettus G, Wendling F, Guye M, Valton L, Régis J, Chauvel P, et al. Enhanced EEG functional connectivity in mesial temporal lobe epilepsy. *Epilepsy Res*. 2008;81(1):58–68.
 19. Dauwels J, Eskandar E, Cash S. Localization of seizure onset area from intracranial non-seizure EEG by exploiting locally enhanced synchrony. *Conf Proc IEEE Eng Med Biol Soc*. 2009;2009:2180–3.
 20. Demuru M, Kalitzin S, Zweiphenning W, van Blooijis D, van't Klooster M, Van Eijsden P, et al. To resect or not to resect? Unbiased performances of single and combined biomarkers in intra-operative corticography for tailoring during epilepsy surgery. medRxiv. <https://doi.org/10.1101/2019.12.26.19015883>
 21. Van Mierlo P, Papadopoulou M, Carrette E, Boon P, Vandenberghe S, Vonck K, et al. Functional brain connectivity from EEG in epilepsy: seizure prediction and epileptogenic focus localization. *Prog Neurobiol*. 2014;121:19–35. <https://doi.org/10.1016/j.pneurobio.2014.06.004>
 22. Pincus SM. Assessing serial irregularity and its implications for health. *Ann N Y Acad Sci*. 2006;954:245–67. <https://doi.org/10.1111/j.1749-6632.2001.tb02755.x>
 23. Costa M, Goldberger AL, Peng C-K. Multiscale entropy analysis of complex physiologic time series. *Phys Rev Lett*. 2002;89(6):68102.
 24. Sato Y, Ochi A, Mizutani T, Otsubo H. Low entropy of interictal gamma oscillations is a biomarker of the seizure onset zone in focal cortical dysplasia type II. *Epilepsy Behav*. 2019;96:155–9.
 25. Ben-Jacob E, Doron I, Gazit T, Rephaeli E, Sagher O, Towle VL. Mapping and assessment of epileptogenic foci using frequency-entropy templates. *Phys Rev E Stat Nonlin Soft Matter Phys*. 2007;76(5 Pt 1):51903.
 26. Gazit T, Doron I, Sagher O, Kohrman MH, Towle VL, Teicher M, et al. Time-frequency characterization of electrocorticographic recordings of epileptic patients using frequency-entropy similarity: a comparison to other bi-variate measures. *J Neurosci Methods*. 2011;194(2):358–73.
 27. Mooij AH, Frauscher B, Amiri M, Otte WM, Gotman J. Differentiating epileptic from non-epileptic high frequency intracerebral EEG signals with measures of wavelet entropy. *Clin Neurophysiol*. 2016;127(12):3529–36.
 28. Klimes P, Duque JJ, Brinkmann B, Van Gompel J, Stead M, St Louis EK, et al. The functional organization of human epileptic hippocampus. *J Neurophysiol*. 2016;115(6):3140–5.
 29. Warren CP, Hu S, Stead M, Brinkmann BH, Bower MR, Worrell GA. Synchrony in normal and focal epileptic brain: the seizure onset zone is functionally disconnected. *J Neurophysiol*. 2010;104(6):3530–9.
 30. Plesinger F, Jurco J, Halamek J, Jurak P. SignalPlant: an open signal processing software platform. *Physiol Meas*. 2016;37(7):N38–48.
 31. Spanedda F, Cendes F, Gotman J. Relations between EEG seizure morphology, interhemispheric spread, and mesial temporal atrophy in bitemporal epilepsy. *Epilepsia*. 1997;38(12):1300–14.
 32. Kullback S, Leibler RA. On information and sufficiency [internet]. *Ann Math Stat*. 1951;22:79–86. <https://doi.org/10.1214/aoms/1177729694>
 33. Gardner AB, Worrell GA, Marsh E, Dlugos D, Litt B. Human and automated detection of high-frequency oscillations in clinical intracranial EEG recordings. *Clin Neurophysiol*. 2007;118(5):1134–43.
 34. Klimes P, Cimbálnik J, Brazdil M, Hall J, Dubeau F, Gotman J, et al. NREM sleep is the state of vigilance that best identifies the epileptogenic zone in the interictal electroencephalogram. *Epilepsia*. 2019;60(12):2404–15.
 35. Roehri N, Pizzo F, Lagarde S, Lambert I, Nica A, McGonigal A, et al. High-frequency oscillations are not better biomarkers of epileptogenic tissues than spikes [internet]. *Ann Neurol*. 2018;83:84–97. <https://doi.org/10.1002/ana.25124>
 36. Cimbálnik J, Klimes P, Sladky V, Nejedly P, Jurak P, Pail M, et al. Multi-feature localization of epileptic foci from interictal, intracranial EEG. *Clin Neurophysiol*. 2019;130(10):1945–53.
 37. Cimbálnik J KPTV. Epycom: ElectroPhYsiology COmputational Module. Available from: <https://gitlab.com/icrc-bme/epycm> [accessed 26 February 2022].
 38. Cimbálnik J, Hewitt A, Worrell G, Stead M. The CS algorithm: a novel method for high frequency oscillation detection in EEG [internet]. *J Neurosci Methods*. 2018;293:6–16. <https://doi.org/10.1016/j.jneumeth.2017.08.023>
 39. Zelmann R, Mari F, Jacobs J, Zijlmans M, Dubeau F, Gotman J. A comparison between detectors of high frequency oscillations. *Clin Neurophysiol*. 2012;123(1):106–16.
 40. Gliske SV, Irwin ZT, Chestek C, Hegeman GL, Brinkmann B, Sagher O, et al. Variability in the location of high frequency oscillations during prolonged intracranial EEG recordings. *Nat Commun*. 2018;9(1):2155.
 41. Karoly PJ, Rao VR, Gregg NM, Worrell GA, Bernard C, Cook MJ, et al. Cycles in epilepsy. *Nat Rev Neurol*. 2021;17(5):267–84.

SUPPORTING INFORMATION

Additional supporting information can be found online in the Supporting Information section at the end of this article.

How to cite this article: Travnicsek V, Klimes P, Cimbálnik J, Halamek J, Jurak P, Brinkmann B, et al. Relative entropy is an easy-to-use invasive electroencephalographic biomarker of the epileptogenic zone. *Epilepsia*. 2023;64:962–972. <https://doi.org/10.1111/epi.17539>